

*Supporting information*

**PVA-based bulk microneedles capable of high insulin loading and pH-triggered degradation for multi-responsive and sustained hypoglycemic therapy**

Yuhong Ma <sup>a,#</sup>, Wei Wang <sup>a,#</sup>, Mujiao He <sup>a</sup>, Yunzhu Liu <sup>a</sup>, Caihua Li <sup>a</sup>, Yinan Zhong <sup>a</sup>, Quanmin Bu <sup>b,\*</sup>, Dechun Huang <sup>a,\*</sup>, Hongliang Qian <sup>a,\*</sup>, and Wei Chen <sup>a</sup>

<sup>a</sup> *Department of Pharmaceutical Engineering, School of Engineering, China Pharmaceutical University, Nanjing 211198, P. R. China.*

<sup>b</sup> *Department of Public Security and Management, Jiangsu Police Institute, Nanjing 210031, Jiangsu, China*

*\* Corresponding authors.*

*E-mail addresses:*

qmbu@sina.com (Q.M. Bu)

cpu hdc@cpu.edu.cn (D.C. Huang)

hlqian@cpu.edu.cn (H.L. Qian)

<sup>#</sup> These authors contributed equally to this work.

## *1. Materials*

Triethylamine (Et<sub>3</sub>N, 99.5%), (3-dimethyl aminopropyl)-ethyl carbodiimide hydrochloride (EDC·HCl), *N*-hydroxysuccinimide (NHS), 3-aminophenyl boronic acid (APBA), 3-mercaptopropane-1, 2-diol (MPD), poly (vinyl alcohol) 205 (PVA, type 205), 3-(4,5-dimethylthiazol)-2,5-diphenyltetrazolium bromide (MTT), fluorescein isothiocyanate (FITC), and polyvinylpyrrolidone (PVP, MW 300 kDa) were obtained from Macklin Biochemical (Shanghai, China). Coomassie brilliant blue, streptozocin (STZ, 98%), and glucose oxidase (GOx) were purchased from Aladdin Chemistry (Shanghai, China). Methacryloylchloride and INS (bovine pancreas, 27 U/mg) were brought from Yuanye Biotechnology (Shanghai, China). All the other reagents and solvents were purchased from Sinopharm Chemical Reagent (Shanghai, China) and used as received. PDMS MN male molds were purchased from Microchip Pharmaceutical Technology (Hangzhou, China). RAW 264.7 cell was offered by the Shanghai cell of the Chinese Academy of Sciences.

## *2. Synthesis of 3-aminophenyl boronic acid (APBA)-decorated PVA-VEMA-COOH (PVA-VEMA-COOH (PBA))*

According to our previous study, the synthesis of vinyl ether methacrylate (VEMA)-functionalized polyvinyl alcohol (PVA-VEMA) and carboxyl-modified polyvinyl alcohol (PVA-VEMA-COOH) was carried out [1]. Furthermore, PVA-VEMA-COOH(PBA) was synthesized by an amination reaction between PVA-VEMA-COOH and APBA. Specifically, PVA-VEMA-COOH (100 mg, COOH units: 0.085 mmol), EDC·HCl (35 mg, 0.18 mmol), and NHS (21 mg, 0.18 mmol) were stirred in DMSO. Subsequently, APBA (9 mg, 0.060 mmol) was introduced and allowed to stir at 37 °C for 8 h. The resulting product (81 mg, yield: 81 %) was transferred to a dialysis bag (MWCO: 3500) to remove APBA for one day, then precipitated in cold diethyl ether, and dried under vacuum at room temperature.

### *3. Synthesis of 3-mercaptopropane-1,2-diol (MPD)-functionalized PVA-VEMA (PVA-VEMA(MPD))*

To synthesize PVA-VEMA(MPD) via the Michael-type conjugate addition reaction, the reaction was conducted in anhydrous DMSO at room temperature under a nitrogen atmosphere. Initially, PVA-VEMA (100 mg, VEMA units: 0.051 mmol) was dissolved in DMSO, and subsequently, MPD (15 mg, 0.038 mmol), and Et<sub>3</sub>N (11 mg, 0.12 mmol) were introduced under nitrogen protection. Following 8 h of stirring at room temperature, the mixture was extensively dialyzed with methanol (MWCO: 3500) for 6 h, concentrated by rotary evaporation, precipitated in cold diethyl ether, and dried under vacuum at room temperature. The yield was found to be 77% (77 mg).

#### *4. Characterization of the Swelling Kinetics of MNs@GI*

The swelling capability of the MNs@GI patch was assessed by immersing it in pH 7.4 PBS with varying glucose concentrations (1 or 4 mg/mL) at 37 °C. The swelling ratio was calculated based on a formula of the weight of the MNs@GI patches:

$$\text{Swelling Ratio} = \frac{W_t - W_0}{W_0}$$

where  $W_t$  represents the weight of the MNs@GI patch at different time points and  $W_0$  represents its initial net weight. Before examination by SEM, the internal structure of the swollen hydrogels was cryo-dried and lyophilized.

### *5. Long-term storage performance of microneedles*

To examine potential alterations in the morphology of microneedles following prolonged storage, microneedles that had been stored for 6 months were retrieved and subjected to visual analysis using a digital camera, to assess the structural integrity of their tips. To further evaluate the bioactivity of insulin within long-term stored microneedles, diabetic mice were administered post-fasting with long-term stored microneedles (MNs@INS and MNs@GI). An equal amount of free insulin was subcutaneously injected as a control. A glucometer (Cofee Medical Technology, Changsha, China) was used to measure blood glucose levels (GLs) at intervals post-administration.

## 6. Biocompatibility analysis

The cytotoxicity of MNs materials to Raw 264.7 cells was determined using an MTT assay. Briefly, Raw 264.7 cells ( $1 \times 10^4$  cells per well) were seeded into 96-well plates and incubated overnight. Afterward, the cells were treated with the MNs solution at concentrations ranging from 0.05 to 1 mg/mL for 24 h. Then, MTT solution in PBS (10  $\mu$ L, 5 mg/mL) was added for another 4 h. Afterward, the cell culture medium was replaced with 150  $\mu$ L of dimethyl sulfoxide (DMSO) to dissolve the formaldehyde completely, and the relative viability of the cells was measured at 562 nm with a microplate reader (Molecular devices spectramax@i3x).

The biocompatibility of the MN patch *in vivo* was evaluated by histological analysis. The mice were euthanized after MNs@INS and MNs@GI percutaneously penetrated the back of mice for 12 h, and the surrounding tissues were removed. Then, the tissues were fixed with 10 % formalin, embedded in paraffin, and sectioned at 5  $\mu$ m, which were further stained using Hematoxylin-eosin (H&E) for histological analysis.

### *7. Long-term efficacy and toxicity studies*

To evaluate the enduring effectiveness and potential harm of individual microneedle, a group of diabetic mice was randomly allocated into three groups, each consisting of three mice. These groups were then subjected to daily administration of PBS, MNs@INS, and MNs@GI for 14 days. Throughout this period, the mice's body weight, water uptake, and food uptake were closely monitored daily. Following the 14-day administration period, blood samples were collected from the mice's tail veins one hour after the last administration, and the levels of proinflammatory cytokines (specifically IL-6, IL-1 $\beta$ , and TNF- $\alpha$ ) were quantified.

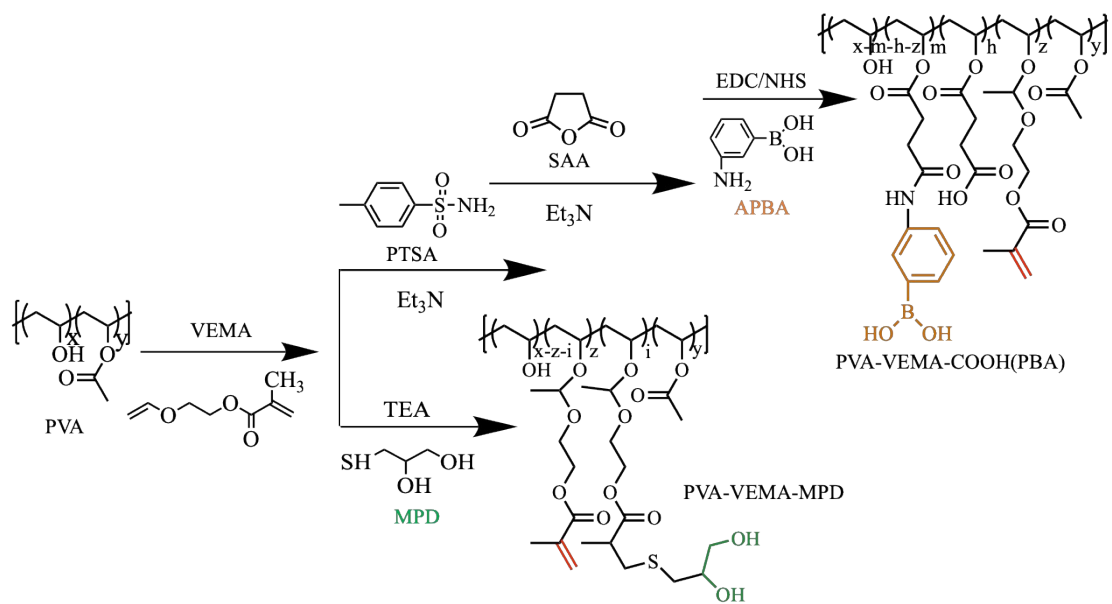


**Table S1** Encapsulation efficiency and loading capacity of MNs@INS and MNs@GI

| Samples | Loading capacity (%) |         | Encapsulation efficiency (%) |         |
|---------|----------------------|---------|------------------------------|---------|
|         | GOx                  | Insulin | GOx                          | Insulin |
| MNs@INS | /                    | 36.4    | /                            | 91.0    |
| MNs@GI  | 17.8                 | 32.5    | 89.0                         | 81.3    |

**Table S2** Pharmacokinetic parameters of subcutaneous (s.c.) administration, MNs@INS, and MNs@GI group.

| Samples    | Dose (U/kg) | AUC (mIU·h/L) | RBA %        |
|------------|-------------|---------------|--------------|
| INS (s.c.) | 40          | 209.5 ± 9.436 | 100          |
| MNs@INS    | 80          | 242.1 ± 13,92 | 57.78 ± 0.69 |
| MNs@GI     | 80          | 355.1 ± 13.07 | 84.75 ± 0.67 |



**Scheme S1** The synthetic pathway employed for the production of PVA-VEMA, PVA-VEMA-COOH(PBA), and PVA-VEMA-MPD.

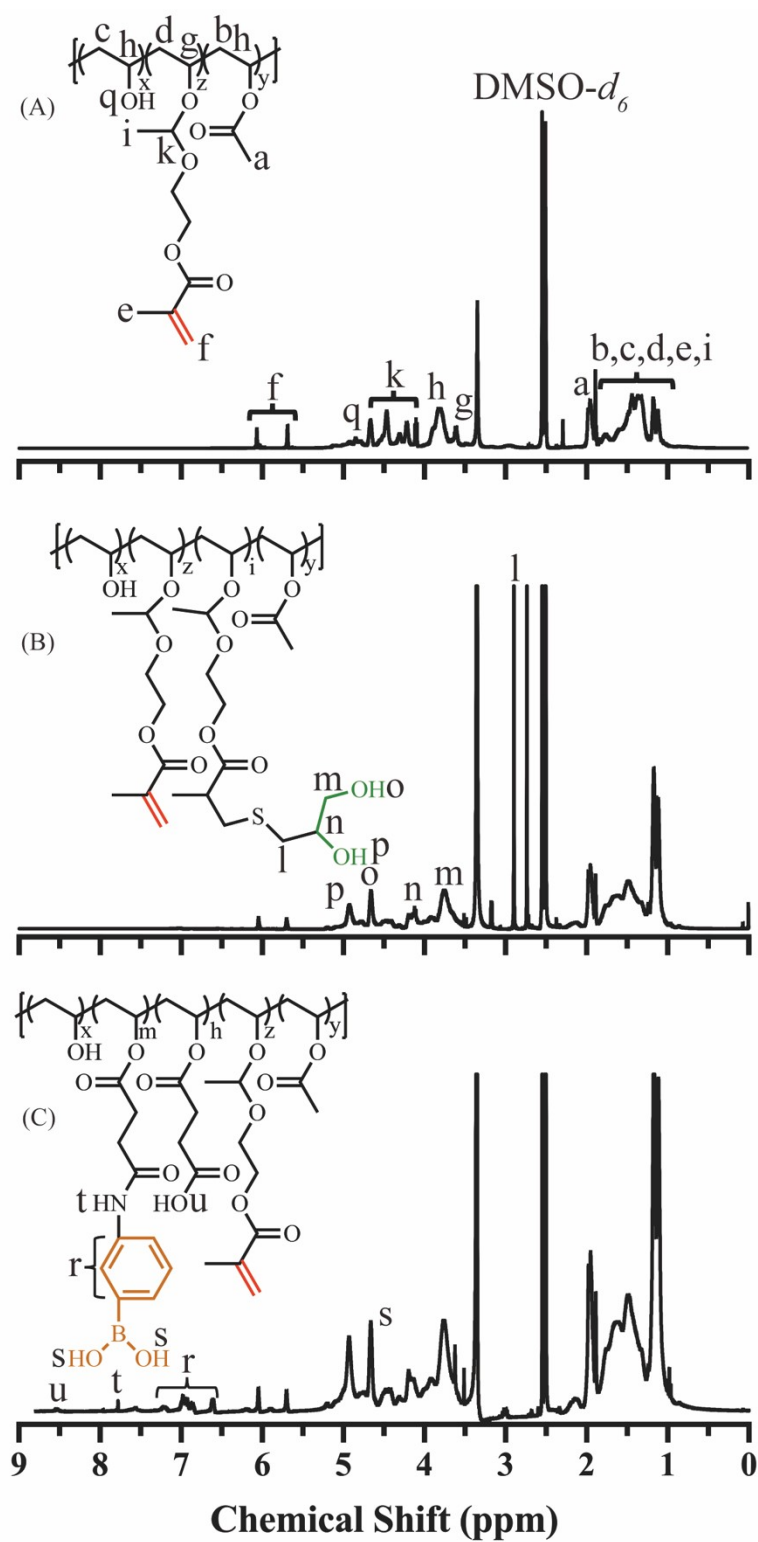


**Fig. S1.** (A) <sup>1</sup>H NMR spectrum of PVA-VEMA in DMSO-*d*<sub>6</sub>; (B) <sup>1</sup>H-NMR spectrum of PVA-VEMA-MPD in DMSO-*d*<sub>6</sub>; (C) <sup>1</sup>H NMR spectrum of PVA-VEMA-COOH(APBA) in DMSO-*d*<sub>6</sub>.

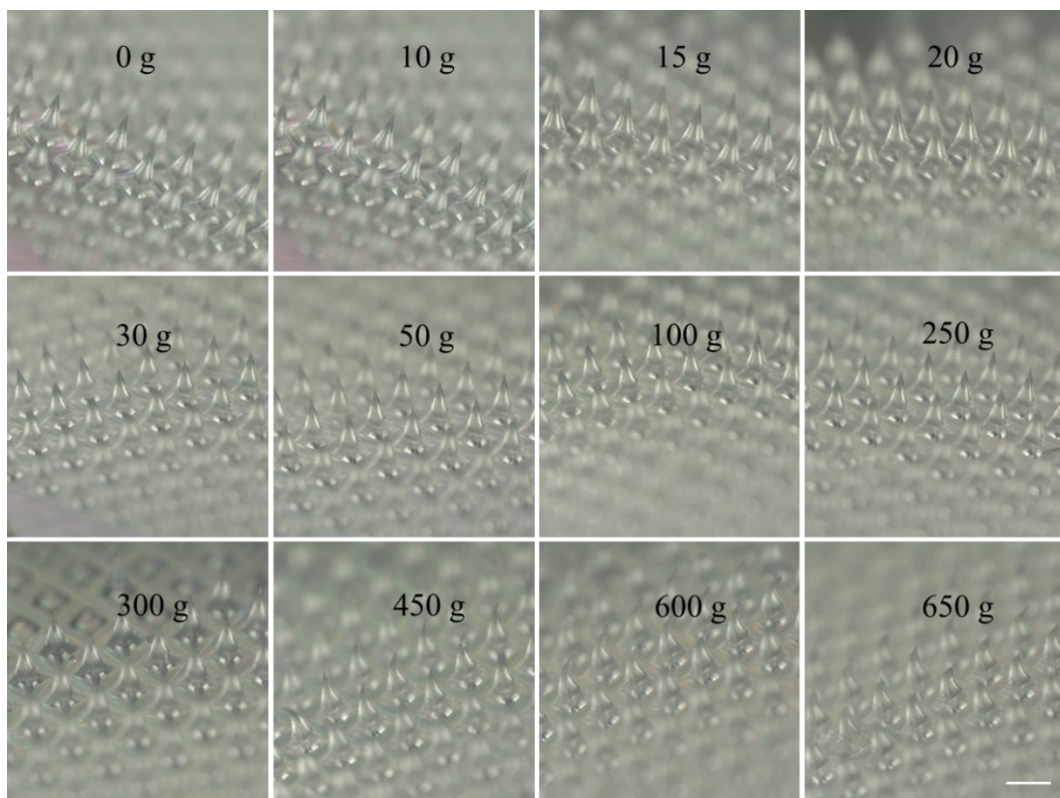


**Fig. S2.** The digital images of MNs@GI treated with different weights, scale bar: 500  $\mu\text{m}$ .

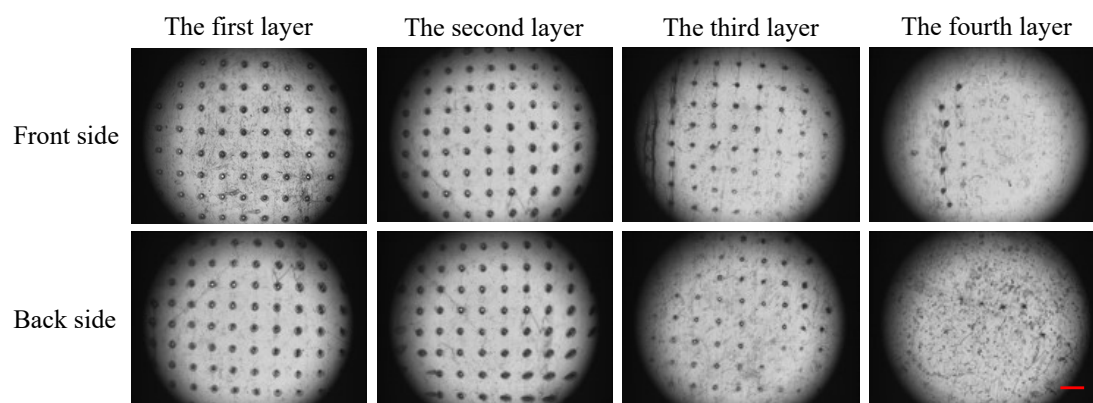


**Fig. S3.** Permeation testing of Parafilm M films, scale bar: 50  $\mu\text{m}$ .

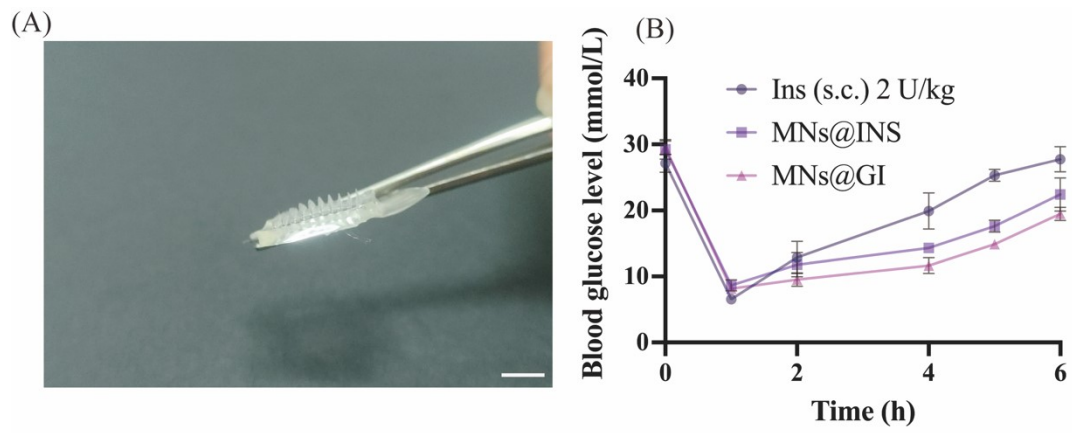


**Fig. S4.** (A) Optical microscope image of long-term storage of MNs@GI, scale bar: 500µm; (B) Blood glucose levels after long-term storage of MNs@GI and MNs@INS administrated to diabetic mice.

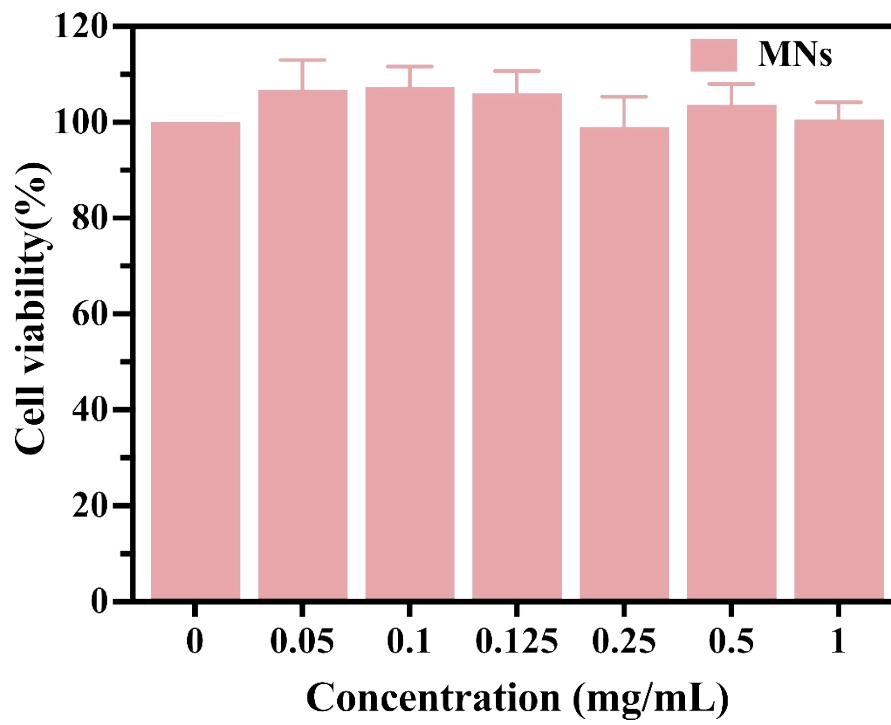


**Fig. S5.** Cytotoxicity of blank MNs after 24 h incubation with RAW 264.7 cells. Error bars indicate SD (n=4).



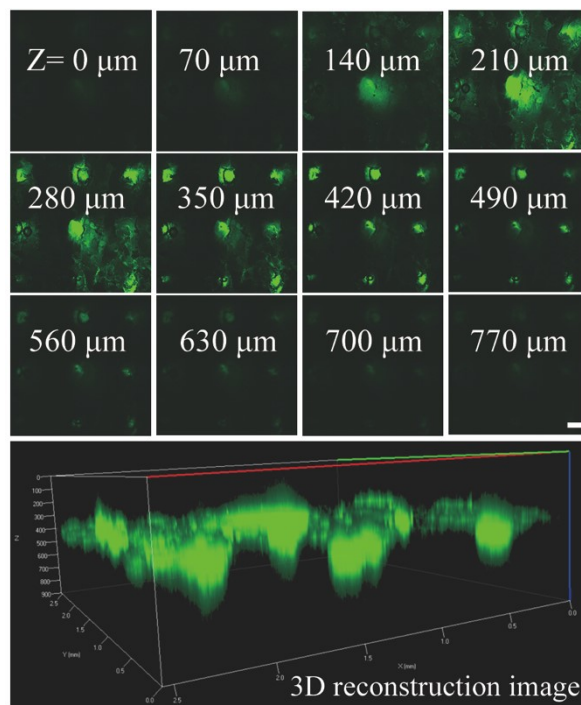


**Fig. S6.** Confocal micrograph and corresponding 3D reconstruction of the skin after 30 min of insertion, scale bar: 200  $\mu\text{m}$ .

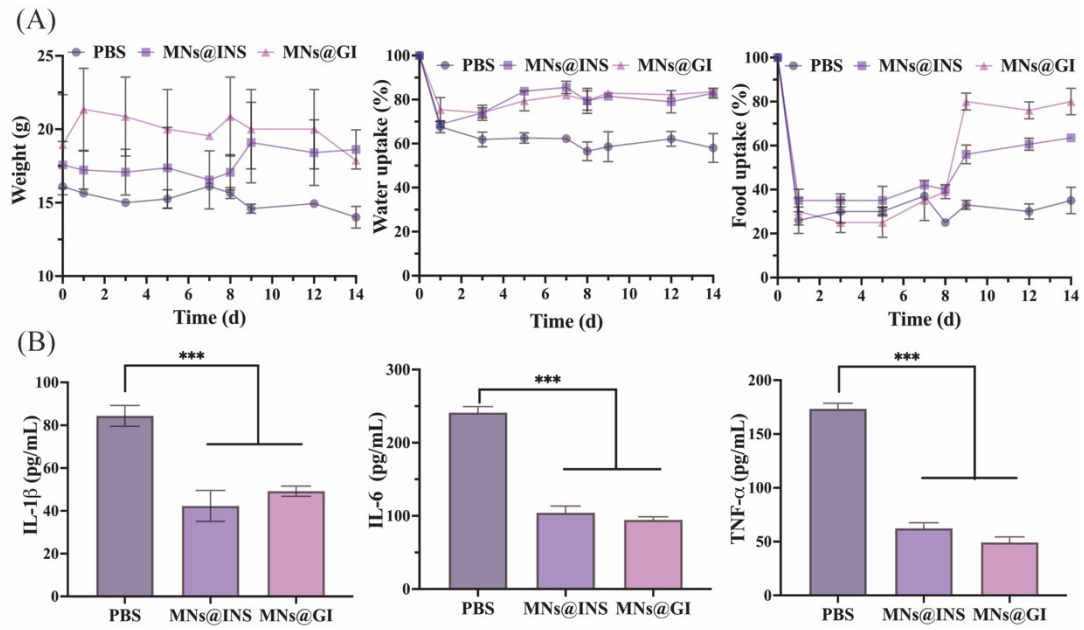


**Fig. S7.** (A) Daily changes in body weight, water uptake and food uptake; (B) Serum levels of TNF- $\alpha$ , IL-6, and IL-1 $\beta$  in mice.

- [1] X. Chen, H. Qian, H. Qiao, B. Dong, E. Chen, D. Huang, T. Wang and W. Chen, *Biomacromolecules*, 2020, 21, 1285–1294.